



Geochemical characterisation and protolith restoration of metamorphic rocks at Lazishao graphite mine, Sichuan

Wenqi Cheng², Haijun Yu^{1,2*}, Xue Wang³, Decai Kong², Bo Long²

1. Sichuan Shu-Neng Mineral Co., Ltd., Leshan, Sichuan, 614600, China;

2. Mine bureau of Sichuan province, 106 geological team, Chengdu, Sichuan, 611130, China;

3. Sichuan Shu-Dao Highway Group Co., Ltd. Chengdu, Sichuan, 610000, China.

* Correspondence: yuhaijun0601@163.com

Abstract: This study determined the deposit characteristics and geochemical features of metamorphic rocks from the Lazishao graphite deposit in order to reconstruct the metamorphic protoliths and palaeo-sedimentary environment. The results show that the SiO₂ content of the metamorphic rocks is high (55.60% to 77.94%), while Na₂O is 0.22% to 1.85%, K₂O is 1.87% to 3.45%, K₂O > Na₂O, and K₂O/Na₂O + K₂O > 0.5. The fractionation degree of light rare earth elements (LREEs) is greater than that of heavy rare earth elements (HREEs), with LREE/HREE ratios of 3.09 to 8.77; La_N/Yb_N is 2.72 to 10.75, with a mean value of 9.69. The rocks have moderate negative Eu anomalies ($\delta\text{Eu} = 0.50$ to 0.89 , mean = 0.64). Ionic lithophile elements (e.g., Rb, Ba, and K) are relatively enriched, but Sr is relatively depleted. The graphite-bearing metamorphic rocks in the study area originated from sedimentary rocks, mainly mudstone and greywacke. The palaeo-sedimentary environment was a low-salinity terrestrial freshwater body in a cold or moderately cold climatic zone.

Keywords: graphite mine; deposit characteristics; geochemical characteristics; carbon source; Lazishao

1. Introduction

Graphite (also known as 'black gold') is one of China's strategic non-metallic mineral resources (Deng ShaoJun, 2020). Graphite has electrical and thermal conductivities similar to those of metallic materials, and desirable plasticity and expandability (Zhang TengFei, 2015). It is widely used in various industrial fields, including metallurgy, mechanics, chemistry, and electricity, and has become a strategic resource for modern cutting-edge technologies (Zhang et al., 2013; Li et al., 2015; Jiang, 2016; Wang et al., 2017).

Graphite mines are widely distributed in China, although those with large-scale output are mainly concentrated in five regions: Shandong, Heilongjiang, Hunan, Inner Mongolia, and Sichuan. Graphite mines in Sichuan Province are mainly distributed in Nanjiang County of Bazhong City and Renhe District and Yanbian County of Panzhihua City. The national resource base (Nanjiang–Wangcang graphite mine) is in Sichuan Province and the graphite mineral resource exploration and development base is in Panzhihua City (Yu et al., 2017; Department of Natural Resources of Sichuan Province, 2017). At present, ultra-large graphite deposits at Zhongba and Tianping in Panzhihua City have been discovered. The metallogenic age of graphite deposits in Panzhihua is mainly Palaeoproterozoic–Mesoproterozoic, and metallogenic processes included the deposition of graphitic rocks, regional metamorphism, and late-stage superposed contact metamorphism (Yu et al., 2020).

However, the microscopic characteristics, geochemistry, ore genesis, carbon source, and other deposit features of graphite mines in the region have not been thoroughly explored. In this study, we investigated the geochemistry of metamorphic rocks from the Lazishao graphite mine (Renhe District, Panzhihua City) in order to determine the metamorphic protoliths and palaeo-sedimentary environment. The results of this study provide a reference for analysing the metallogenic mechanism and genesis of sedimentary–metamorphic graphite deposits in the Panxi area of Sichuan Province and across China.



47 **2. Regional geological background**

48 **2.1. Geotectonic position**

49 The study area is in the central Yangzi Craton (Kangdian axis), east of the Songpan–Ganzi
 50 orogenic belt, and at the northeast tip of the Gondwana palaeo-continent. This region forms an
 51 important part of the Panxi metallogenic belt (Fig. 1a). The Kangdian basement fault uplift zone
 52 is a horst-like structure composed of Archaean to Early Mesozoic metamorphosed magmatic
 53 complexes with a banded distribution. Magmatic rocks are primarily Jinning granites of the
 54 Chengjiang period, whose extension is controlled by north–south trending faults. The primary
 55 metallogenic belt is the Fe–Cu–V–Ti–Ni–Sn–Pb–Zn–Au–Pt–rare earth–asbestos metallogenic
 56 belt along the Yangtze metallogenic province of the Kangdian fault uplift zone; the secondary
 57 metallogenic belt is the Cu–Ni–Pb–Zn–graphite sub-metallogenic belt of the Yanbian
 58 palaeo-forearc basin.

59 **2.2. Geological characteristics of the mining area**

60 The regional stratigraphy is simple, mainly consisting of the second member of the
 61 Lengzhuguan Formation (Kangding Group), the first member of the Neoproterozoic Guanyinya
 62 Formation, and the first member of the Cenozoic Yuanyongjing Formation. The second member
 63 of the Lengzhuguan Formation is the ore-bearing formation of the graphite deposits, whose
 64 lithology is mainly sericite (muscovite)–quartz schist and two-mica–quartz schist. During the
 65 massive intrusion of monzonitic granites in the Cryogenian, most schists of the Lengzhuguan
 66 Formation were removed, leaving only a small number of lenticular and strip-shaped outcrops
 67 of the Lengzhuguan Formation in the west(Fig. 1b).

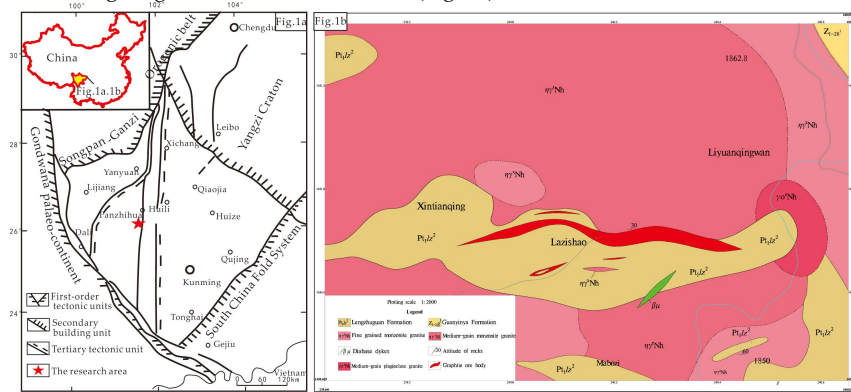


Fig.1 Geotectonic location and geological map of the research area(Wang Xue , 2014)

68 **3. Petrographic characteristics**

69 **3.1. Ore types**

70 Natural graphite deposits at Lazishao are mainly sericite–quartz schist; some graphite
 71 infills between quartz grains and some is arranged parallel to mica and quartz flakes, showing a
 72 schistose texture. Graphite flake sizes are 48–680 μm and the ore is a crystalline flake graphite.

73 **3.2. Ore characteristics**

74 The ore mineral is graphite; gangue minerals are mainly quartz, muscovite, and sericite,
 75 with occasional biotite and feldspar; metal minerals mainly include magnetite, hematite,
 76 limonite, pyrrhotite, and pyrite. Fresh graphite surfaces are black, and weathered surfaces are
 77 brownish-black. Granular minerals such as quartz (anhedral) and a small amount of feldspar
 78 (anhedral to subhedral) are distributed in the ore, while flaky minerals, including graphite and
 79 mica, have a directional arrangement among the granular minerals. Flaky minerals are less
 80 abundant than granular minerals, exhibiting a grano-lepidoblastic texture with a predominantly
 81 schistose structure (Fig. 2 and Fig. 3) following the banded structure. The graphite content is
 82 about 10% and mostly comprises individual flakes or flake aggregates. Graphite particles are



83 generally 0.2 to 0.6 mm in length and 0.05 to 0.1 mm in width. Graphite is mostly in banded and
84 directional, extending along the same direction as muscovite and biotite, and graphite grains
85 are evenly distributed among the quartz grains (Fig. 4). Euhedral columnar minerals are
86 occasionally seen. The quartz content is ~60%, and particles are anhedral and granular with a
87 small grain size (< 0.8 mm), showing a mosaic structure. Quartz grains have been deformed
88 under stress, with flattened and elongated morphology, displaying wavy extinction and optical
89 anomalies; however, the long axis of quartz grains is still in a directional arrangement with
90 flaky minerals. Mica is mostly muscovite and sericite, with a small amount of biotite. Muscovite
91 and sericite (flake diameters 0.05 to 1.9 mm mm) have a silky lustre and typically represent 20%
92 of the sample; the content of muscovite is higher than that of sericite. The biotite content is
93 relatively low (generally 2% to 5%) and grains are unevenly distributed. Biotite particles are
94 usually brown and flaky, generally 0.25 to 0.6 mm in diameter, and have a directional
95 arrangement. Metallic minerals account for 0.1% to 3% and are unevenly distributed in the ore.
96 Magnetite accounts for ~90% of the metallic minerals, followed by pyrite, with occasional
97 arsenopyrite and chalcopyrite. These minerals are generally interstitial between the particles of
98 major minerals.



Fig.2 Graphite aligned along the foliation plane



Fig.3 Flake structure of graphite ore

99

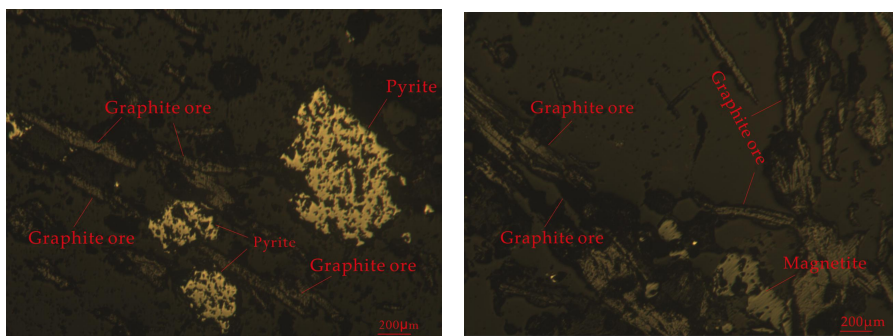


Fig.4 Oriented Graphite ore (polished section10×10)

100

3.3. Ore-fixed carbon content



101 The fixed carbon content of graphite ores in the study area ranges from 2.03% to 18.87%,
 102 and the average fixed carbon content of industrial-grade ores in the mining area is 5.16%, with
 103 the fixed carbon occurring in graphite. The fixed carbon content of muscovite (sericite)-quartz
 104 schist is mainly ~1%. There is little fixed carbon in the of granites and gangue rocks, and the
 105 distribution of fixed carbon content in the deposit is irregular.

106 *3.4. Graphite flake size*

107 Graphite flake size determines the quality of graphite products. Based on the analysis of 22
 108 samples, graphite flakes in the mining area are generally between 0.048 and 0.68 mm. Graphite
 109 flakes of +100 mesh account for 17% to 80%, with an average of 52.4%; 100 to 80 mesh graphite
 110 flakes account for 9% to 28%, with an average of 19.4%; 80 to 50 mesh graphite flakes account
 111 for 5% to 35%, with an average of 19.8%; graphite flakes of > 50 mesh account for 3% to 38%,
 112 with an average of 13.3%. Graphite flake size increases with depth, making the deep orebody
 113 more favourable than the surface orebody.

114 **4. Materials and methods**

115 A total of 11 fresh samples were collected from drill holes, including seven graphite ore
 116 samples and four mica-quartz schist samples. Samples were analysed at the Mineral Testing
 117 Centre of Xichang, Sichuan Provincial Bureau of Geology and Mineral Exploration and
 118 Development (Table 1).

119 Table 1 Analysis of Lazishao Graphite Mine Samples

Analytical object	Analytical method	Analytical accuracy
Major elements	X-ray fluorescence spectrometry	Better than 0.1% to 1.0%
V ₂ O ₅ and Fe ₂ O ₃	Inductively coupled plasma-atomic emission spectrometry	Reproducibility up to 5%
Trace elements and rare earth elements	Inductively coupled plasma-mass spectrometry (ICP-MS)	Better than 10%

120 **5. Results**

121 *5.1. Geochemical characteristics of major elements*

122 Major elements compositions of the graphite ore and mica-quartz schist are shown in
 123 Table 2. The SiO₂ content is generally high, ranging from 55.60% to 77.94%, with an average of
 124 68.74%, which is higher than the average SiO₂ content in the upper crust (66%) (Deng ShaoJun,
 125 et al.,2020). Na₂O show little variation, ranging from 0.22% to 1.85%, with an average of 0.68%,
 126 while K₂O ranges from 1.87% to 3.45%, with an average of 2.70%. In all samples, K₂O > Na₂O,
 127 and K₂O/Na₂O + K₂O > 0.5 (4.64–12.31, with an average of 8.32), indicating that the protoliths of
 128 the graphite deposit and mica-quartz schist were of normal sedimentary origin (He Tongxing
 129 et al.,1980). TiO₂ ranges from 0.14% to 1.36% (average of 0.44%), MgO ranges from 0.59% to
 130 5.11%, and CaO ranges from 0.14% to 3.22%. In all samples, CaO < MgO, which also indicates
 131 that the metamorphic protoliths had a normal sedimentary origin (He Tongxing et al.,1980).
 132 The Fe₂O₃ content is 2.43% to 3.92%, with an average of 2.99%; FeO ranges from 0.50% to 5.50%,
 133 with an average value of 2.52; Al₂O₃ ranges from 5.45% to 14.81%, with an average of 9.96%. The
 134 SiO₂/Al₂O₃ ratio is between 3.75 and 13.84 (7.96–13.84 for the seven graphite ore samples and
 135 3.75–4.69 for the four mica-quartz schist samples), with an average of 7.85%. This shows that
 136 the maturity levels of the seven graphite ore samples are similar, and those of the four
 137 mica-quartz schist samples are similar (Feng Wei, 2019). SiO₂ is significantly negatively



138 correlated with Al_2O_3 . P_2O_5 ranges from 0.072% to 0.92%, which is generally low, and MnO is
139 between 0.010% and 0.090%, with a small variation range.

140 On Harker diagrams (Fig. 5), SiO_2 is negatively correlated with Al_2O_3 , Na_2O , K_2O , TiO_2 ,
141 CaO , MnO , MgO , and Fe_2O_3 , and positively correlated with P_2O_5 and V_2O_5 . On this basis, the
142 chemical differentiation of the rocks is constrained by sedimentary differentiation (He et
143 al.,1980; Long , 2016).

144
145

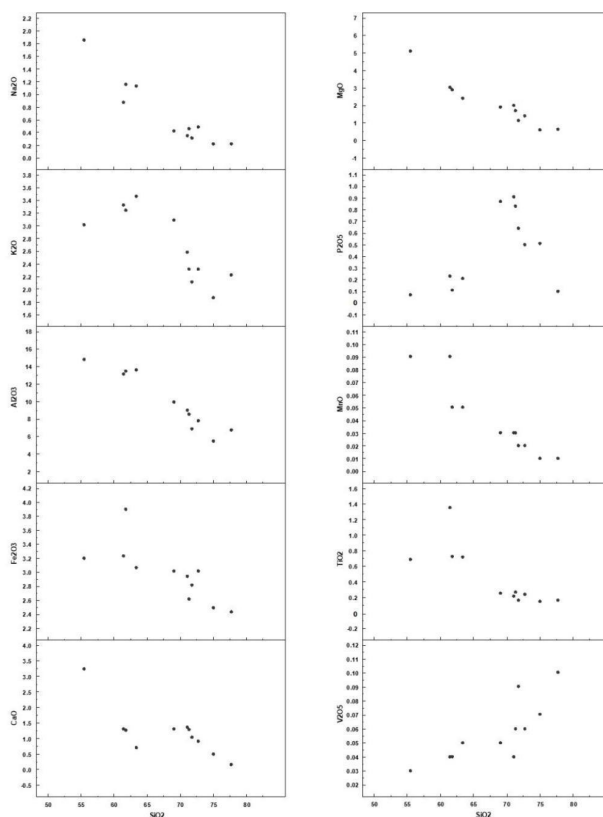


Fig.5 Harker diagrams for the Lazishao Graphite mine

146



147

Table 2 Results of major elements analysis of Lazishao graphite deposit metamorphic rocks (wt.%)

sample number	sample type	Na ₂ O	K ₂ O	SiO ₂	Al ₂ O ₃	Fe ₂ O ₃	CaO	MgO	MnO	V ₂ O ₅	TiO ₂	P ₂ O ₅	FeO	H ₂ O ⁺	loss on ignition	TOTAL
LZS-BZY-01	mica-quartz schist sample	1.85	3.01	55.60	14.81	3.20	3.22	5.11	0.087	0.035	0.68	0.072	5.09	2.58	4.77	100.11
LZS-BZY-02	mica-quartz schist sample	1.16	3.26	62.21	13.49	3.92	1.27	2.89	0.046	0.043	0.72	0.112	4.00	2.00	5.38	100.50
LZS-SMK-01	graphite ore sample	0.34	2.61	72.00	9.05	2.97	1.37	2.00	0.027	0.039	0.21	0.920	1.50	1.42	6.72	101.18
LZS-SMK-02	graphite ore sample	0.48	2.33	73.50	7.84	3.04	0.91	1.40	0.023	0.062	0.23	0.503	1.33	0.70	8.60	100.95
LZS-SMK-03	graphite ore sample	0.22	2.22	77.94	6.72	2.43	0.14	0.61	0.010	0.106	0.16	0.109	0.59	0.96	7.98	100.18
LZS-SMK-04	graphite ore sample	0.22	1.87	75.41	5.45	2.50	0.48	0.59	0.013	0.071	0.14	0.514	0.50	0.70	12.02	100.47
LZS-SMK-05	graphite ore sample	0.42	3.10	69.63	9.98	3.03	1.31	1.91	0.026	0.048	0.25	0.883	1.33	1.38	7.40	100.69
LZS-SMK-06	graphite ore sample	0.31	2.12	72.28	6.90	2.83	1.04	1.14	0.021	0.090	0.16	0.642	1.42	1.00	10.64	100.59
LZS-SMK-07	graphite ore sample	0.45	2.33	72.19	8.56	2.64	1.29	1.72	0.027	0.058	0.26	0.842	1.92	1.40	7.38	101.07
LZS-BZY-03	mica-quartz schist sample	1.12	3.45	63.18	13.53	3.05	0.69	2.37	0.049	0.046	0.71	0.219	4.59	1.94	4.68	99.62
LZS-BZY-04	mica-quartz schist sample	0.88	3.36	62.16	13.25	3.27	1.30	3.05	0.090	0.039	1.36	0.230	5.50	2.16	4.44	101.09

148

Table 3 Rare earth elements analysis results of Lazishao graphite deposit metamorphic rocks and relevant parameter value (ppm)

sample number	sample type	La	Ce	Pr	Nd	Sm	Eu	Gd	Tb	Dy	Ho	Er	Tm	Yb	Lu	ΣREE	LRREE	HRREE	LREE/LHREE	La _N /Yb _N	δEu	δCe
LZS-BZY-01	mica-quartz schist sample	36.6	70.1	8.64	32.6	6.36	1.33	4.49	0.96	6.68	1.62	4.31	0.71	4.09	0.64	179.13	155.63	23.50	6.62	6.42	0.72	0.93
LZS-BZY-02	mica-quartz schist sample	61.1	114.3	14.6	51.87	9.69	1.69	6.94	1.44	9.90	2.43	6.12	1.01	5.58	0.85	286.83	252.56	34.27	7.37	7.85	0.59	0.91
LZS-SMK-01	graphite ore sample	35.6	88.3	10.3	41.0	9.54	1.59	7.43	1.69	12.4	3.24	8.54	1.41	8.40	1.32	230.72	186.33	44.39	4.20	3.04	0.56	1.12
LZS-SMK-02	graphite ore sample	26.9	36.9	7.52	31.8	7.44	1.30	6.10	1.37	10.0	2.65	6.8	1.12	7.10	1.06	148.06	111.86	36.20	3.09	2.72	0.57	0.63
LZS-SMK-03	graphite ore sample	19.7	27.3	5.06	20.5	4.45	1.13	2.99	0.59	0.65	1.09	2.80	0.56	3.32	0.50	94.64	78.14	16.50	4.74	4.26	0.89	0.65
LZS-SMK-04	graphite ore sample	30.2	35.5	7.94	33.1	7.05	1.29	4.55	1.00	5.05	1.11	2.82	0.44	5.51	0.40	132.96	115.08	17.88	6.44	8.63	0.65	0.55
LZS-SMK-05	graphite ore sample	47.6	112.4	13.8	52.6	11.16	2.8	8.54	1.86	12.7	3.14	7.7	1.27	7.43	1.18	283.38	239.56	43.82	5.47	4.60	0.63	1.07
LZS-SMK-06	graphite ore sample	27.2	39.1	8.12	34.4	8.00	1.29	6.42	1.27	8.50	2.06	4.99	0.79	4.76	0.66	147.56	118.11	29.45	4.01	4.10	0.53	0.64
LZS-SMK-07	graphite ore sample	40.5	82.6	11.3	45.2	9.89	1.43	7.12	1.50	10.4	2.59	6.12	1.6	6.53	1.07	227.85	190.92	36.93	5.17	4.45	0.50	0.93
LZS-BZY-03	mica-quartz schist sample	56.5	106.3	13.7	49.48	9.76	1.43	6.43	1.26	8.01	1.81	4.46	0.68	3.77	0.57	263.73	236.74	26.99	8.77	10.75	0.65	0.92
LZS-BZY-04	mica-quartz schist sample	45.4	89.0	11.5	42.8	8.76	1.91	6.24	1.29	8.71	2.12	5.55	0.84	4.69	0.71	229.52	199.37	30.15	6.61	6.94	0.75	0.93



149

Table 4 Trace element analysis results of Lazishao graphite deposit metamorphic rocks (ppm)

sample number	sample type	Rb	Ba	Th	U	K	Ta	Nb	La	Ce	Sr	Nd	P	Zr	Hf	Sm	Ti	Y
LZS-BZY-01	mica-quartz schist sample	162.00	620.00	10.40	1.82	25000.00	1.47	10.50	36.60	70.10	80.80	32.60	316.80	255.00	6.11	6.36	4100.00	40.00
LZS-BZY-02	mica-quartz schist sample	167.00	800.00	18.60	2.65	27100.00	1.66	14.60	61.10	114.00	40.90	51.60	484.00	276.00	6.00	9.87	4300.00	61.60
LZS-SMK-01	graphite ore sample	136.00	530.00	9.62	4.02	21700.00	1.93	6.82	35.60	88.30	13.90	41.00	4048.00	267.00	6.12	9.54	1300.00	78.20
LZS-SMK-02	graphite ore sample	103.00	480.00	9.47	7.56	19300.00	1.61	6.52	26.90	36.90	12.00	31.80	2200.00	141.00	3.65	7.44	1400.00	66.70
LZS-SMK-03	graphite ore sample	84.10	330.00	6.15	6.27	18400.00	1.80	6.28	19.70	27.30	9.25	20.50	440.00	154.00	4.17	4.45	1000.00	26.90
LZS-SMK-04	graphite ore sample	70.00	420.00	6.41	4.88	15500.00	0.38	3.34	30.20	35.50	11.10	33.10	2244.00	181.00	3.45	7.05	840.00	29.50
LZS-SMK-05	graphite ore sample	142.00	650.00	11.50	6.41	25700.00	0.94	8.03	47.60	112.00	27.40	52.80	3872.00	244.00	6.50	11.60	1500.00	74.30
LZS-SMK-06	graphite ore sample	79.00	400.00	8.30	5.44	17600.00	0.64	4.81	27.20	39.10	8.80	34.40	2816.00	171.00	3.41	8.00	1000.00	50.60
LZS-SMK-07	graphite ore sample	102.00	460.00	8.66	4.57	19300.00	1.35	8.68	40.50	82.60	17.70	45.20	3696.00	201.00	5.51	9.89	1600.00	63.20
LZS-BZY-03	mica-quartz schist sample	184.00	850.00	14.20	3.57	28600.00	10.70	17.00	56.50	106.00	56.00	49.70	924.00	314.00	4.00	9.48	4300.00	44.90
LZS-BZY-04	mica-quartz schist sample	195.00	670.00	11.50	2.83	27900.00	1.56	16.50	45.40	89.00	63.50	42.80	1012.00	253.00	3.06	8.76	8200.00	52.10
sample number	sample type	Yb	Lu	Ni	Cr	Co	al	fm	c	alk	si	Zr	Zr/Ti O2	al-a lk	La/ Th	Rb/ Sr	Sr/B a	/
LZS-BZY-01	mica-quartz schist sample	4.09	0.64	48.90	322.00	25.40	14.79	16.67	3.22	4.86	25.92	255.00	375.00	9.93	3.52	2.00	0.13	/
LZS-BZY-02	mica-quartz schist sample	5.58	0.85	69.80	89.20	22.50	13.42	14.71	1.26	4.39	28.89	276.00	383.33	9.03	3.28	4.08	0.05	/
LZS-SMK-01	graphite ore sample	8.40	1.32	77.40	39.90	29.70	8.94	9.37	1.35	2.92	33.21	267.00	1271.43	6.02	3.70	9.78	0.03	/
LZS-SMK-02	graphite ore sample	7.10	1.06	108.00	62.30	17.50	7.77	8.75	0.90	2.79	33.98	141.00	613.04	4.98	2.84	8.58	0.03	/
LZS-SMK-03	graphite ore sample	3.32	0.50	28.70	51.40	17.60	6.71	6.07	0.14	2.44	36.31	154.00	962.50	4.27	3.20	9.09	0.03	/
LZS-SMK-04	graphite ore sample	2.51	0.40	78.20	62.80	16.30	5.42	6.08	0.48	2.08	35.02	181.00	1292.86	3.34	4.71	6.31	0.03	/
LZS-SMK-05	graphite ore sample	7.43	1.18	98.20	65.40	28.00	9.91	9.27	1.30	3.50	32.27	244.00	976.00	6.41	4.14	5.18	0.04	/
LZS-SMK-06	graphite ore sample	4.76	0.66	112.00	48.80	17.10	6.86	8.18	1.03	2.42	33.53	171.00	1068.75	4.44	3.28	8.98	0.02	/
LZS-SMK-07	graphite ore sample	6.53	1.07	99.20	43.00	21.00	8.47	8.85	1.28	2.76	33.33	201.00	773.08	5.71	4.68	5.76	0.04	/
LZS-BZY-03	mica-quartz schist sample	3.77	0.57	63.80	92.70	23.90	13.58	13.16	0.69	4.58	29.60	314.00	442.25	9.00	3.98	3.29	0.07	/
LZS-BZY-04	mica-quartz schist sample	4.69	0.71	65.70	74.50	25.30	13.11	15.01	1.29	4.19	28.70	253.00	187.41	8.92	3.95	3.07	0.09	/

150



151 5.2. Geochemical characteristics of rare earth elements

152 Rare earth element (REE) data of the 11 samples are shown in Table 3. Total REE (Σ REE)
 153 ranges from 94.64 to 286.83 ppm, with an average of 202.22 ppm; total light REE (Σ LREE)
 154 ranges from 78.14 to 252.56 $\mu\text{g/g}$, with an average of 171.3 $\mu\text{g/g}$; total heavy REE (Σ HREE)
 155 ranges from 16.50 to 44.39 $\mu\text{g/g}$, with an average of 30.92 $\mu\text{g/g}$. The LREE/HREE ratio is 3.09 to
 156 8.77, and $\text{La}_N/\text{Yb}_N = 2.72$ to 10.75, with an average of 9.69. These results indicate a degree of
 157 fractionation between LREEs and HREEs, suggesting that the metamorphic protoliths were
 158 sedimentary rocks. Eu anomalies (δEu) range from 0.50 to 0.89, with a mean value of 0.64, and
 159 there are no significant δC (0.55–1.12) anomalies.

160 Chondrite-normalised LREE patterns (Fig. 6) are right-skewed, while HREE curves are
 161 relatively gentle. All samples show significant negative Eu anomalies, and LREE contents are
 162 much higher than those of chondritic standard values, consistent with the REE distribution
 163 pattern in the khondalite series at the margin of the Yangzi plate. This indicates that the
 164 metamorphic protoliths were sedimentary rocks and claystone; the low-maturity metamorphic
 165 rock series originated from continental crust basement with protoliths composed of sandy and
 166 argillaceous clastic sediments of early Proterozoic immature source areas (Liu XinXin, 2015).

167 North American shale-normalised REE patterns (Fig. 7) show relatively gentle curves, with
 168 individual samples showing negative Ce anomalies. There are also slightly positive Ho
 169 anomalies, relative LREE enrichment, relative HREE depletion, negative Eu anomalies, and
 170 slightly negative Ce anomalies. Such characteristics are consistent with river, lagoon, and
 171 marginal sea sediments (Deng , 2020 ; Wildman T R et al., 1973; Zhao , 1997; Piper D Z,
 172 1985; Goldstein S J et al., 1988; Murray R W et al., 1991; Sholkovitz E R, Jacobson S B et
 173 al.,1994).

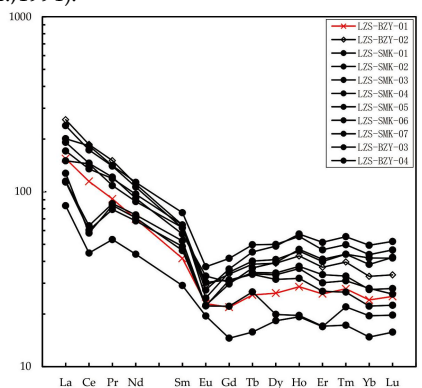


Fig.6 Chondrite-normalized REE patterns for Lazishao Graphite mine(Boynton W V, 1984)

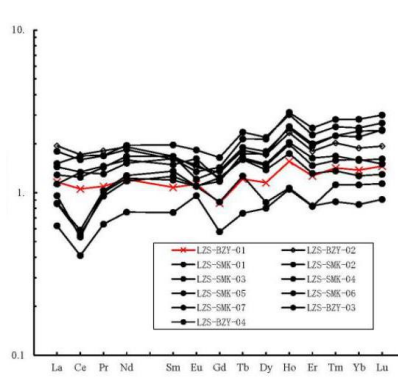


Fig.7 North American Shale normalized REE patterns for Lazishao Graphite mine(Haskin L A, et al., 1968)

174 5.3. Geochemical characteristics of trace elements

175 Trace element data are shown in Table 4. Large ion lithophile element (LILE) Rb ranges
 176 from 70 to 195 ppm, with an average of 129.0 ppm; Ba ranges from 330 to 850 ppm, with an
 177 average of 564.5 ppm; K ranges from 15,500 to 28,600 ppm, with an average of 22,372.73 ppm; Sr
 178 ranges from 8.80 to 80.8 ppm, with an average of 31.0 ppm. High field strength element (HFSE)
 179 Th varies little, ranging from 6.15 to 18.6ppm, with an average of 10.4 ppm; Nb ranges from 3.34
 180 to 71.0 ppm, with an average of 9.40 ppm; Ta is relatively low, ranging from 6.15 to 18.6 ppm,
 181 with an average of 10.4 ppm; P varies widely from 316.8 to 4048.0 ppm, with an average of
 182 2004.8 ppm; Zr ranges from 141 to 314 ppm, with an average of 223.0 ppm; Hf ranges from 3.06
 183 to 6.50 ppm, with an average of 4.73 ppm; La/Th ranges from 2.84 to 4.71, with a mean value of
 184 3.75. As Sr is relatively enriched in marine sedimentary environments, the Rb/Sr ratio can be
 185 used to distinguish marine and terrestrial sediments (Liang Shuai, 2015). Here, Rb/Sr ranges
 186 from 2.00 to 9.78 (with a mean value of 6.01); all values are > 1, indicating that the sediments are



187 well sorted and probably originated from a terrestrial depositional environment. Sr/Ba varies in
 188 a relatively small range of 0.02 to 0.13, with a mean value of 0.05.

189 A spider diagram of trace element ratios relative to original mantle source values (Fig. 8)
 190 shows relative LILE enrichment (e.g., Rb, Ba, and K) and obvious Sr depletion. HFSE, such as
 191 Nb and Ta, show slight depletion, while Zr, Hf, and Th are relatively balanced, with gentle
 192 curves. The content of all elements, except Sr and Ti, are higher than the original mantle source
 193 values.

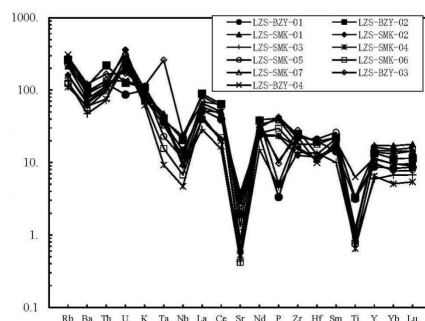


Fig 8 Trace elements primitive mantle standard element cobweb diagram of Lazishao graphite deposit (Sun S S, Mc Donough W F. 1989)

194 **6. Discussion**

195 *6.1. Metamorphic protoliths*

196 The Lazishao graphite deposit has undergone multiple phases of tectonic deformation and
 197 metamorphism, with superposed foliations and mineral assemblages. As such, accurate
 198 recreation of metamorphic protoliths cannot be accomplished merely based on geological
 199 features in the field, mineral assemblages, or mineralogical characteristics; geochemical data are
 200 also needed.

201 Owing to strong activity of the major components (e.g., SiO₂), their contents can change
 202 during multi-phase metamorphism, reducing the accuracy of protolith recreation. Instead,
 203 Winchester et al. (1980) chose relatively inactive elements (Zr, Ti, and Ni) to construct a
 204 Zr/TiO₂-Ni diagram. As shown in Fig. 9, data from the four mica-quartz schist samples and
 205 seven graphite ore samples were projected into the zone of sedimentary rocks on a Zr/TiO₂-Ni
 206 diagram, suggesting that the metamorphic protoliths of the Lazishao graphite deposit were
 207 sedimentary rocks, and that graphite-bearing metamorphic rocks in the study area are
 208 para-metamorphic.

209 Simonen (1953) used an Al+fm-C+alk-Si diagram to demonstrate the chemical
 210 characteristics of different metamorphic rocks, and showed wide variations in Al, fm, C, and alk.
 211 Simonen's diagram can effectively eliminate the effects of Si variation on protolith restoration.
 212 Numerous studies have verified that Simonen's diagram performs well in the determining
 213 metamorphic protoliths.

214 Based on the data in Table 4, Simonen's diagram was plotted for the Lazishao graphite
 215 deposit (Fig. 10). Volcanic rocks plot in the centre, argillaceous sedimentary rocks plot in the
 216 upper left, sandy sedimentary rocks plot in the upper right, and calcareous sedimentary rocks
 217 plot in the lower left. There is no apparent boundary between argillaceous sedimentary and
 218 sandy sedimentary rock zones. All 11 samples projected into the argillaceous sedimentary rock
 219 zone, confirming that the protoliths of the metamorphic rocks in the study area were
 220 sedimentary and that the metamorphic rocks are para-metamorphic.

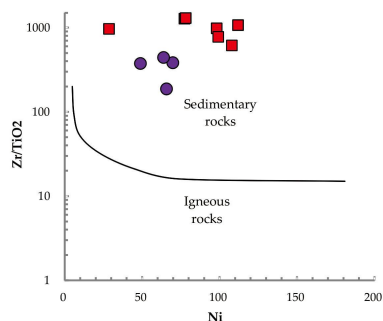


Fig 9 Diagram of Zr/TiO₂-Ni of Lazishao graphite deposit(Wang Renmin et al., 1986)

(● are mica-quartz schist samples, ■ are graphite ore samples)

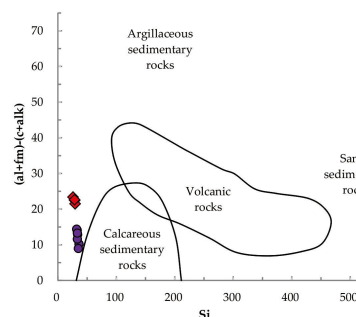


Fig 10 Diagram of al+fm+c+alk-Si of Lazishao graphite deposit(Wang Renmin et al., 1986)

(● are graphite ore samples, ◆ are mica-quartz schist samples)

221 REEs are incompatible; that is, they cannot enter the crystal structures of rock-forming
 222 minerals or form independent mineral phases. As such, REEs are relatively stable and are not
 223 easily altered by metamorphism or metasomatism, making them suitable for reconstructing
 224 metamorphic protoliths (Meng Hui, 2015). On a La/Yb-ΣREE diagram (Fig. 11) (Allegre C T,
 225 1978), the 11 samples mostly plot in the shale, claystone, and sandstone zones, providing
 226 further evidence that the protoliths of graphite-bearing metamorphic rocks in the study area
 227 were sedimentary rocks, and that the metamorphic rocks are para-metamorphic.

228 Leake (1969) proposed the (Al-alk)-C diagram to distinguish metasedimentary and
 229 metavolcanic rocks. On an (Al-alk)-C diagram (Fig. 12), the Lazishao graphite samples plot in
 230 the feldspathic claystone and greywacke zones, confirming that the metamorphic protoliths
 231 were feldspathic claystone and greywacke sedimentary rocks.

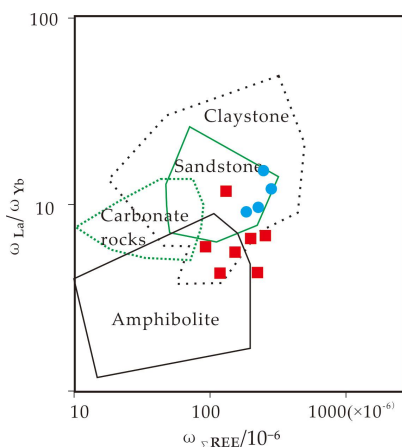


Fig 11 Diagram of La/Yb-ΣREE of Lazishao graphite deposit(Wang Renmin et al., 1986)

(● are mica-quartz schist samples, ■ are graphite ore samples)

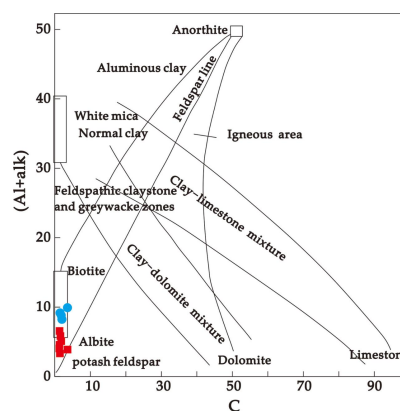


Fig 12 Diagram of (al-alk)-c of Lazishao graphite deposit(Wang Renmin et al., 1986)

(● are mica-quartz schist samples, ■ are graphite ore samples)



233 In summary, the protoliths of metamorphic rocks in the Lazishao graphite deposit were
 234 sedimentary rocks, primarily comprised of mud shale and mixed greywacke.

235 6.2. Palaeo-sedimentary environment

236 Rocks formed in different depositional environments differ in terms of mineral
 237 composition and the contents and ratios of specific elements (Zhao Zhenhua, 1997). Since the
 238 protoliths of the Lazishao graphite deposit were mainly mud shale and greywacke, we infer
 239 that the corresponding depositional environment was a terrestrial or low-energy static shallow
 240 water environment.

241 The ternary diagram of claystone composition in different climatic zones and the Ba-Sr
 242 diagram proposed by Melezhik and Predovsky (1982) are widely used for distinguishing
 243 claystone depositional environments and palaeo-climatic conditions (Fig. 13). Here, the sample
 244 predominantly plot in the terrestrial facies zone of a cold or moderately cold climate of the
 245 ternary diagram; this is supported by the relatively high SiO₂ and K₂O, which are indicative of
 246 cold or moderately cold climate. On a Ba-Sr diagram (Fig. 14), almost all sample points plot in
 247 the freshwater environment zone.

248 In summary, the palaeo-sedimentary environment of the metamorphic protoliths was a
 249 low-salinity terrestrial freshwater body in a cold or moderately cold climatic zone. Combined
 250 with the geochemical characteristics of REEs, we speculate that the sedimentary environment of
 251 the Lazishao graphite deposit was a low-energy static water environment of the fluvial-lagoon
 252 facies.

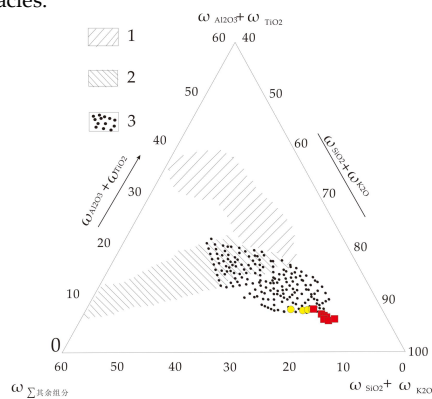


Fig 13 Composition diagram of clay rocks in different climatic zones of Lazishao graphite deposit (Wang Renmin et al., 1986)

1-Terrestrial facies clay compositions in humid and hot climatic zones; 2-Marine facies, lacustrine and lagoon facies clay compositions in dry climatic zones; 3-Terrestrial facies clay compositions in cold or moderately cold climatic zones

(● are mica-quartz schist samples, ■ are graphite ore samples)

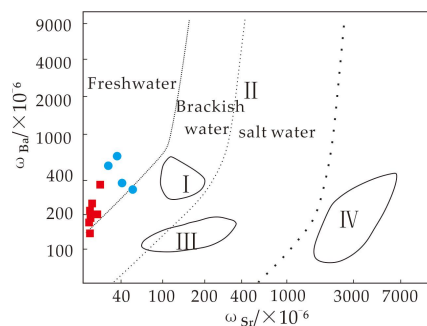


Fig 14 Diagram of Ba-Sr of Lazishao graphite deposit (Wang Renmin et al., 1986)

I -Clay in modern deltaic facies brackish water environment; II -Pelagic sediments of the Pacific Ocean; III-Marine facies carbonate rocks on the Russian platform of different ages; IV-Modern deposits in a high-salinity waterbody

(● are mica-quartz schist samples, ■ are graphite ore samples)

253 6.3. Provenance based on geochemical properties

254 Provenance analysis can reveal the location and properties of sediment sources, paths of
 255 sediment transport, and characteristics of sedimentation and tectonic evolution of the basin. The
 256 clastic components and structure of clastic rocks can also directly reflect the tectonic setting of
 257 the provenance area and the sedimentary basin (Liu BaoJun et al., 2006)

258 The Ni-TiO₂ diagram proposed by Floyd et al. (1989) is very accurate in discriminating the
 259 provenance of metamorphic protoliths. On this diagram (Fig. 15), all seven graphite ore samples
 260 plot in the sandstone zone, two of the four mica-quartz schist samples plot in the argillaceous
 261 rock zone, one plots in the felsic rock zone, and one plots between the argillaceous rock and



262 sandstone zones. Together, this suggests that the provenance of the metamorphic rocks and
 263 graphite ore in the study area is probably argillaceous rock and sandstone.

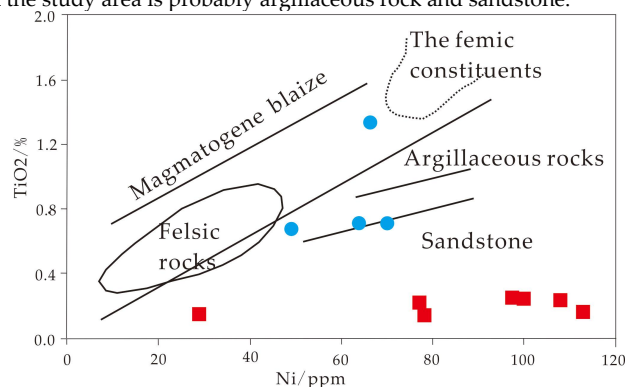


Fig 15 Diagram of Ni-TiO₂ of Lazishao graphite deposit

(● are mica-quartz schist samples, ■ are graphite ore samples)

264

265

266

267

268

269

270

271

272

The La/Th-Hf diagram (Fig. 16) proposed by Floyd and Leveridge (1987) was adopted to further verify the provenance of the graphite-bearing metamorphic rocks. All 11 samples plot within the mixed felsic-intermediate source zone. On the Th-Hf-Co ternary diagram proposed by Taylor and McLennan (1985) (Fig. 17), all 11 samples plot within the upper crust region.

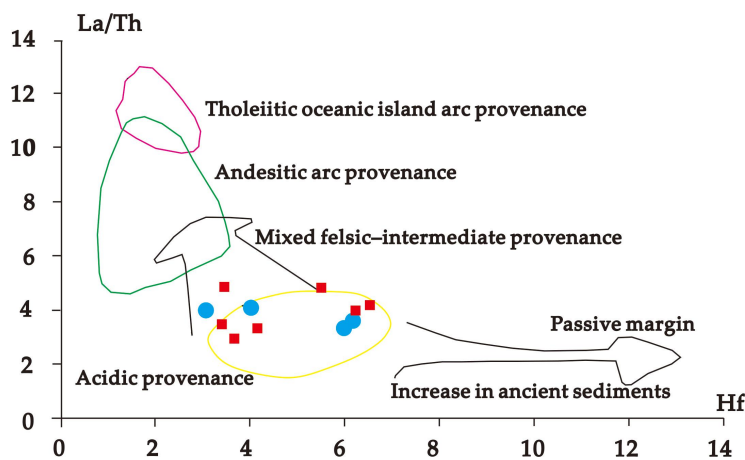


Fig 16 Diagram of La/Th-Hf of Lazishao graphite deposit

(● are mica-quartz schist samples, ■ are graphite ore samples)

273

274

275

276

277

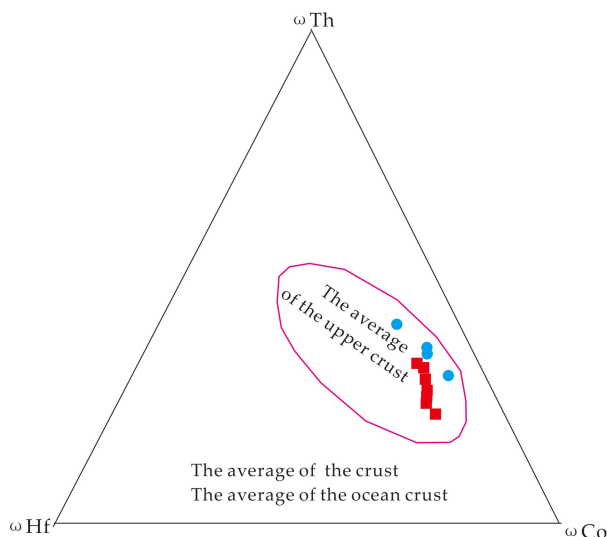


Fig 17 Diagram of Th-Hf-Co of Lazishao graphite deposit

(● are mica-quartz schist samples, ■ are graphite ore samples)

278
279
280
281
282
283
284
285
286
287
288
289
290
291
292
293
294
295
296

In summary, the Lazishao graphite deposit originated from the upper crust, with the main components being argillaceous rock and sandstone from a felsic-intermediate source area.

6.4 Tectonic environment

The discrimination formula $Al_2O_3/(Al_2O_3+Fe_2O_3)$ of Jewell and Stallard (1991) is commonly used to determine geotectonic setting during the deposition of sedimentary rocks. An $Al_2O_3/(Al_2O_3+Fe_2O_3)$ ratio between 0.6 and 0.9 indicates a continental margin environment, a ratio between 0.4 and 0.7 indicates a pelagic environment, and a ratio between 0.1 and 0.4 indicates a mid-ocean ridge environment. The $Al_2O_3/(Al_2O_3+Fe_2O_3)$ ratios of the samples from the Lazishao graphite deposit range from 0.69 to 0.82, with an average of 0.76 (Table 5), indicating a continental margin environment, which is consistent our other results. Similarly, on a K_2O/Na_2O-SiO_2 diagram [37] (Fig. 18), all seven graphite ore samples and plot in the passive continental margin region, three of the four mica-quartz schist samples plot in the active continental margin region, and one of the four mica-quartz schist samples plots in the island arc region.

Table 5 $Al_2O_3/(Al_2O_3+Fe_2O_3)$ of Lazishao graphite deposit

sample number	LZS-BZ Y-01	LZS-BZ Y-02	LZS-S MK-0 1	LZS-S MK-0 2	LZS-S MK-0 3	LZS-S MK-0 4	LZS-S MK-0 5	LZS-S MK-0 6	LZS-S MK-0 7	LZS-BZ Y-03	LZS-BZ Y-04
sample type	mica-quartz schist sample	mica-quartz schist sample	graphite ore sample	graphite ore sample	graphite ore sample	graphite ore sample	graphite ore sample	graphite ore sample	graphite ore sample	mica-quartz schist sample	mica-quartz schist sample
$Al_2O_3/(Al_2O_3+Fe_2O_3)$	0.82	0.77	0.75	0.72	0.73	0.69	0.77	0.71	0.76	0.82	0.80

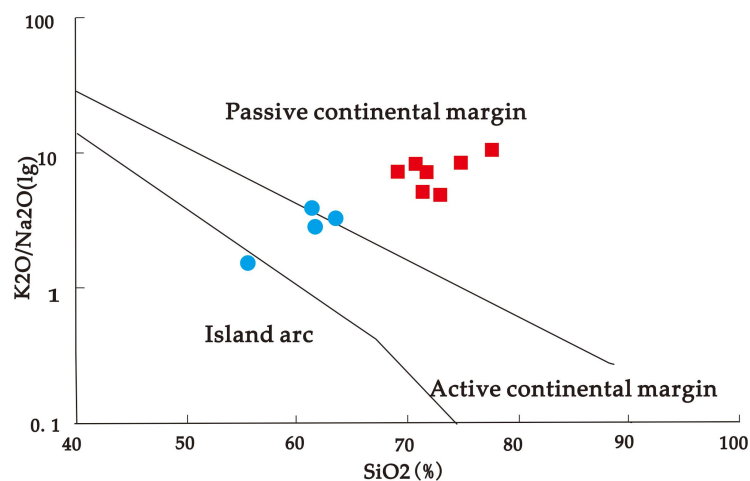


Fig 18 Diagram of K₂O/Na₂O–SiO₂ of Lazishao graphite deposit

(● are mica–quartz schist samples, ■ are graphite ore samples)

297

298

299

300

301

302

303

304

In summary, protoliths of the metamorphic rocks were deposited along a passive continental margin that remained stable for a sufficient period to form a low-energy freshwater environment in which organic-rich claystone and greywacke were deposited. These deposits were then subjected to regional metamorphism, during which organic carbon was recrystallised into graphite.

305

7. Conclusions

306

1. The metamorphic rocks of the Lazishao graphite deposit mainly belong to the second member of the Lengzhuguan Formation of the Kangding Group; their lithology is mainly sericite (muscovite)–quartz schist and two-mica–quartz schist.

309

2. SiO₂ in the Lazishao metamorphic rocks is generally high, ranging from 55.60% to 77.94%; K₂O > Na₂O, and K₂O/(Na₂O+K₂O) > 0.5; fractionation of LREEs > fractionation of HREEs; there are moderate negative Eu anomalies; ionic lithophile elements (Rb, Ba, and K) are relatively enriched, but Sr is prominently depleted.

313

3. Lithogeochemical analysis shows that the metamorphic protoliths of the graphite deposit were sedimentary rocks whose lithology was dominated by carbonaceous claystone and greywacke.

314

315

4. The palaeo-sedimentary environment was a low-salinity terrestrial freshwater body in a cold or moderately cold climatic zone. Sediments were sourced from the upper crust, and the main provenance components were argillaceous rock and sandstone from a felsic–intermediate source area.

317

318

319

5. Tectonic discrimination diagrams suggest that protoliths of the metamorphic rocks in the study area were probably deposited in an organic-rich fluvial–lagoon facies environment on a continental margin; organic-rich claystone and greywacke were deposited over a long period and then subjected to regional metamorphism during which organic carbon was recrystallised into graphite.

320

321

322

323



324 **References**

- 325 Allgre C T. 1978. Quantitative models of trace elements. *Earth Plant Sci Lett*, 38: 1-25.
- 326 B.E.Leake.1969.The discrimination of ortho and paracharnockitic rocks, anothosites and
327 amphibolites.The *Indian Mineralogist*, vol.10,pp.89-104.
- 328 Boynton W V. 1984. Geochemistry of the Rare Earth Elements: meteorite Studies. In: Henderson,
329 p. (Ed),Rare Earth Element Geochemistry[M]. Amsterdam:Elsevier Sci. Publ. Co. , 63-114.
- 330 Department of Natural Resources of Sichuan Province.2017.Overall Plan of Mineral Resources of
331 Sichuan Province (2016-2020)[R].
- 332 Deng ShaoJun.2020.Study on Geological and Geochemical Characteristics and Genesis of
333 Nanjiang Pinghe Graphite Deposit, Sichuan Province[D].Southwest University of Science
334 and technology.
- 335 Deng ShaoJun, ZHU YuYin, LI HuJie.2020. Protolith Recovery and Discussion on
336 Paleosedimentary Environment of Pinghe Graphite Metamorphic Rocks in Nanjiang[J].
337 Journal of Southwest University of Science and Technology, 35(01): 25-29.
- 338 Feng Wei. 2019. Geochemistry and Metallogeny of the Daliangzikou graphite deposit in Laiyang
339 Country,Shandong province[D]. Chang'an University.
- 340 Floyd P A, Winchester JA, Park RG .1989. Geochemistry and tectonic setting of Lewisian clastic
341 metasediments from the Early Proterozoic Loch Maree Group of Gairloch, NW Scotland.
342 *Precambrian Res* 45:203-214.
- 343 Floyd P A, Leveridge B E. 1987. Tectonic environment of the Devonian Gramscatho basin, south
344 Cornwall: framework mode and geochemical evidence from turbiditic sandstones[J].*Journal*
345 *of the Geological Society*, 144(4): 531-542.
- 346 Goldstein S J and Jacobsen S B. 1988. Rare earth elements in river waters [J]. *Earth and Planetary*
347 *Science Letters*, 89:35-47.
- 348 He Tongxing, Lu Liangzhao, Li Shuxun, et al.1980. Petrology of metamorphic rocks [M]. Beijing:
349 Geological Publishing House.
- 350 Haskin L A, Haskin M A, Frey F A, et al. 1968. Relative and absolute terrestrial abundances of the
351 rare earths Relative and absolute terrestrial abundances of the rare earths, Origin and
352 Distribution of the Elements[C]//Ahrens, L. H (Ed.), *Origin and Distribution of the Elements*.
353 Oxford: Pergamon, 889-911.
- 354 Jiang GuangMing. 2016. Geological characteristics and economic and technical evaluation of
355 Nanjiang Graphite deposit in Sichuan Province[J].*New Technology & New Products of*
356 *China*08:130-138.
- 357 Jewell P W. Stallard R F. 1991. Geochemistry and paleoceanographic setting of central
358 Nevada bedded barites[J]. *The Journal of Geology*. 151-170.
- 359 Li Chao, WANG DengHong, ZHAO Hong, et al. 2015. Minerogenetic regularity of graphite
360 deposits in China[J].*Mineral deposits*, 34(06):1223-1236.
- 361 Long Tao.2016.The geochemical characteristics and deposit genesis analysis of Liu Mao graphite
362 deposit in Ji Xi County of Hei Long jiang Province[D].China University of Geosciences
363 (Beijing).
- 364 Liu XinXin. 2015. Chronology,Geochemical characteristics and Genesis of the Xiaodouling
365 graphite deposit in Xichuan county, Henan province[D]. China University of Geosciences
366 (Beijing).
- 367 Liang Shuai. 2015. Genisis Studies of typical crystalline Graphite deposits, In *The North China*[D].
368 Liaoning Technical University.
- 369 Liu BaoJun,HAN ZuoZhen,YANG RenChao.2006. Progress prediction and consideration of the
370 research of modern sedi mentology.*Special Oil and Gas Reservoirs*: 13 (5) : 1-9.
- 371 Murray R W, Brink M R and Brumsack H J, et al. 1991. REE in Japen Sea sediments and diagenetic
372 behavior of Ce/Ce*:Results from ODP Log 127 [J]. *Geochim Cosmochim Acta*, 55: 2453-2466.
- 373 Meng Hui.2015.The geochemical characteristics and deposit genesis analysis of Liu ge Zhuang
374 graphite deposit in Pingdu County of Shandong Province[D].China University of
375 Geosciences (Beijing).
- 376 Melezhik and Predovsky. 1982, Ге химия раннепротерозойской литогенеза, М.« Наука ».
- 377 Piper D Z. 1985. Rare earth elements in the sedimentary cycle:a summary [J]. *Chem Geol*,
378 14:285-304.
- 379 Sun S S, Mc Donough W F. 1989. Chemical and isotopic systematic of oceanic basalts: Implications
380 for mantle composition and processes[A]. In:Sanrder A D and Norry M J, eds. *Magmatism in*
381 *the ocean basins*[C]. Geological Society of London Special Publication. 42:313-345.



- 382 Simonen A. 1953. Stratigraphy and Sedimentation of the Sveco fennidic, early Archean
383 Supracrustal Rocks in Southwestern Finland. *Bull. Comm [J]. Geol. Finlande*, No160, p. 1-64.
384 Sholkovitz E R, Jacobson S B. 1994. Ocean particle chemistry: the fractionation of REE between
385 suspended particles and sea water [J]. *Geochim Cosmochim Acta*. 58:1567-1579.
386 Taylor S R, McLennan S M. 1985. *Oxford: S M. The Continental Crust: Its Composition
387 and Blackwell[M]*. 1-312.
388 Wildman T R and Haskin L A. 1973. Rare Earth in Precambrian Sediments [J]. *Geochim.
389 Cosmochim Acta*, Vol.37, No.3, pp.419-438.
390 Winchester J A Park R G et al. 1980. The geochemistry of Lewisian semipelitic schists from the
391 Gairloch District, western Ross [J]. *Scottish Journal of Geology*, 16(2):165-179.
392 Wang Renmin, He Gaopin, Chen Zhenzhen, et al. 1986. Graphical discriminant method for
393 protolith of metamorphic rocks [M]. Beijing: Geological Publishing House.
394 Wang Li, Fan Junlei, Feng Yangwei. 2017. Graphite Resources Status Quo and Distribution of
395 Graphite Deposits in China [J]. *COAL GEOLOGY OF CHINA*, 29(07): 5-9.
396 Wang Xue. 2014. Geological Characteristics and Prospecting Directions of the Jinsuoqiao Iron Gold
397 Deposit in Huidong, Sichuan [D]. Chengdu University of Technology.
398 Yu Haijun, LI Fan, Xiang Hui, et al. 2017. Research Report on Comprehensive Zoning and Planning
399 Zoning of Mineral Resources Development and Utilization in Sichuan
400 Province [R]. Chengdu: Mine bureau of Sichuan province, 106 geological team
401 Yu Haijun, WANG Xue, BAI Jiaquan. 2020. Main Ore-controlling Structural Characteristics and
402 Prospecting Model of Panzhihua Graphite Deposit [J]. *SiChuan Nonferrous Metal*. 04:33-35.
403 Zhang Tengfei. 2015. The geochemical characteristics and deposit genesis analysis of Xiao
404 chagou graphite deposit in Zhenping County of Henan Province [D]. China University of
405 Geosciences (Beijing).
406 Zhang Lingyan, Wang Hao, Guan Junfang, et al. 2013. Study On Process Mineralogy Of The
407 Graphite In Nanjiang County Sichuan Province [J]. *MINING & METALLURGY*, 95-100.
408 Zhao Zhenhua. 1997. Principle of Trace Elements Geochemistry [M]. Beijing: Science Press.

409 **Disclaimer/Publisher's Note:** The statements, opinions and data contained in all publications are solely
410 those of the individual author(s) and contributor(s) and not of Copernicus Publications and/or the editor(s).
411 Copernicus Publications and/or the editor(s) disclaim responsibility for any injury to people or property
412 resulting from any ideas, methods, instructions or products referred to in the content. The contact author
413 has declared that none of the authors has any competing interests